I&EC research
Industrial & Engineering Chemistry Research

Article

Cite This: Ind. Eng. Chem. Res. 2020, 59, 7174−7181

pubs.acs.org/IECR

CO_2 Absorption from Gas Turbine Flue Gas by Aqueous Piperazine with Intercooling

Tianyu Gao and Gary T. Rochelle*

McKetta Department of Chemical Engineering, The University of Texas at Austin, 200 E. Dean Keeton Street, C0400, Austin, Texas 78712-1589, United States

Supporting Information

ABSTRACT: Amine scrubbing is the most mature technology for postcombustion carbon capture. Much bench- and pilot-scale work has been focused on CO_2 capture from coal-fired flue gas. Because natural gas is inexpensive and readily available in the United States and other countries, the natural gas combined-cycle (NGCC) has been replacing coal for electricity generation. Carbon capture for NGCC is therefore an important technology for the modern power plants. The Piperazine (PZ) Advanced Stripper (PZAS) technology has been established as a benchmark system for second-generation amine scrubbing for CO_2 capture from coal-fired flue gas. It has a fast absorption rate, good energy performance, and strong resistance to thermal degradation and oxidation. PZAS was operated with simulated NGCC flue gas (4.3 mol % (dry) CO_2) at the National Carbon Capture Center (NCCC) in Wilsonville, Alabama in 2019. This paper presents the absorber performance and model validation for the campaign. The absorber was tested with in-and-out and with pump-around intercooling. The variable operating conditions included lean loading (0.19−0.25 m CO_2/mol alkalinity), gas temperature (40, 78 °C), and intercooling temperature (35, 40 °C). Using 5 m PZ CO_2 removal from 82% to 96% was achieved with intercooling and only 12 m of packing. A rigorous, rate-based absorber model accurately predicted the CO_2 removal and temperature profile. The model shows that the delta loading of the solvent at NGCC conditions for 90% removal is greater than at coal conditions, but high CO_2 removal (99%) is more difficult to achieve with NGCC gas than with coal-fired flue gas. The pump-around intercooling was effective, and the intercooling temperature had a large impact on the absorber performance. With pump-around, the delta loading penalty for hot gas feed into absorber without a direct contact cooler was less than 5%.

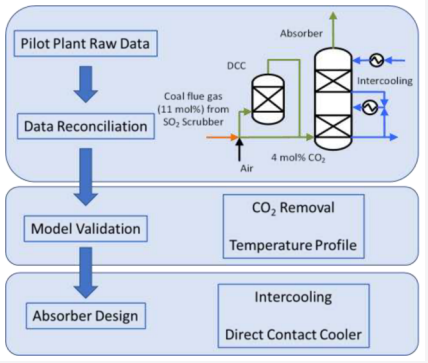

1. INTRODUCTION

In the US, carbon emissions from the power sector accounted for the second largest portion (27.5%) of the total emissions, following transportation (28.9%), in 2017.[1] In the electricity sector coal and natural gas produce 65% and 33% of the carbon emissions, respectively. Natural gas contains less carbon than coal and results in less carbon emission per unit of electricity. In countries where gas is readily available, gas has been replacing coal in the power sector for both economic and environmental reasons. In the US, natural gas usage for power generation surpassed coal in 2016 and currently provides approximately 33% of the electricity. In December 2018, the US Environmental Protection Agency (EPA) proposed a GHG emission regulation for new, modified, and reconstructed power plants. It is projected that most of the fossil fuel electricity-generating capacity additions in the US through 2050 will be Natural Gas Combined-Cycle (NGCC). Therefore, carbon capture for gas application is an important pathway to carbon neutrality for modern power plants.

Various second-generation (2G) amine solvents and processes have been tested for CO_2 capture from coal flue gas (~12 mol % CO_2). With the fast absorption, good energy performance, and high resistance to thermal and oxidative degradation, piperazine (5 m, 30 wt % PZ) with the Advanced Stripper (PZAS) has been demonstrated as a benchmark 2G amine scrubbing process.[2] The process has been tested in the pilot plants at the Separations Research Program (SRP) of the University of Texas at Austin and at the National Carbon Capture Center (NCCC). At SRP, over 2000 h of operation through seven campaigns have tested the 0.43-in. ID absorber with in-and-out and spray intercooling using synthetic flue gas.[3−6] The CO_2 content was varied between 3.5% and 20 mol % for different applications.[6−9] In 2018, PZAS was tested at the NCCC for about 2000 h of operation with coal flue gas (11 mol % CO_2). 90−99% CO_2 removal was achieved with 12 m packing and simple in-and-out intercooling.[10,11]

Previous research work and pilot demonstrations have shown the feasibility of CO_2 capture from coal flue gas.[10,12] The low CO_2 content in NGCC flue gas is a challenge for many technologies, and only a few pilot-scale demonstrations

Special Issue: Carbon Capture and Utilization

Received: October 16, 2019
Revised: December 11, 2019
Accepted: December 18, 2019
Published: December 18, 2019

DOI: 10.1021/acs.iecr.9b05733
Ind. Eng. Chem. Res. 2020, 59, 7174−7181

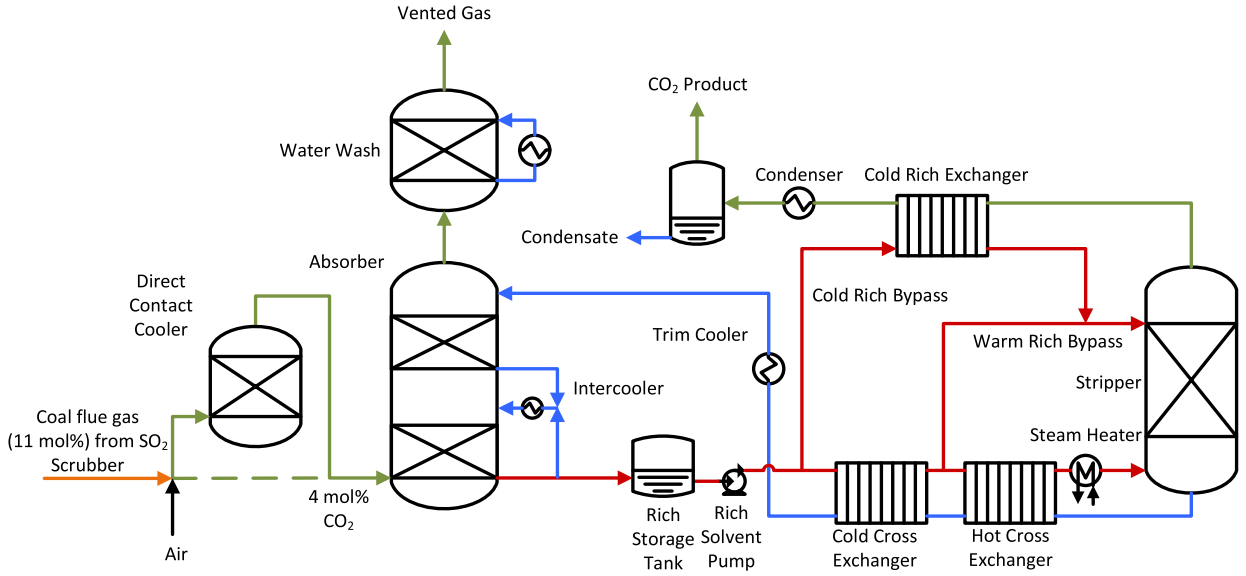

Figure 1. Process flow diagram PZAS tested at NCCC.

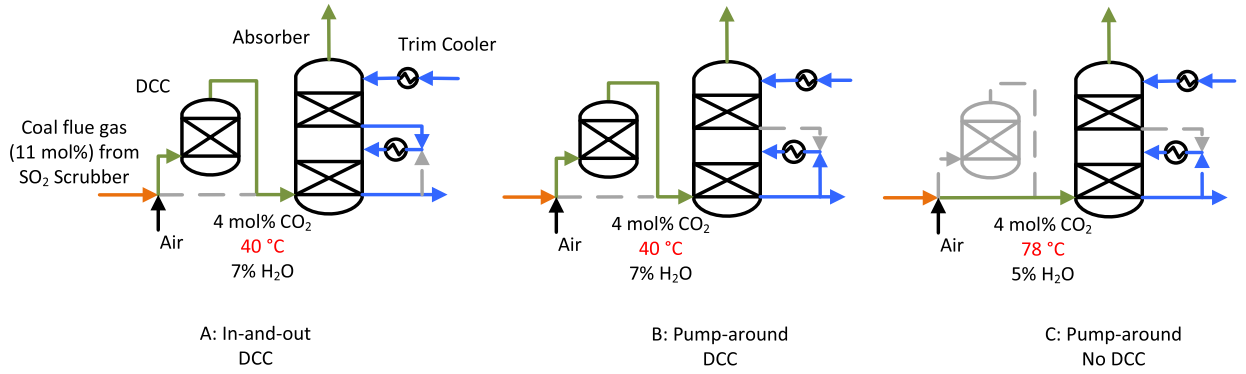

Figure 2. Three configurations of absorber tested during the 2019 pilot plant campaign.

or research can be found in the open literature.[7,13−20] Fluor deployed a commercial NGCC capture plant in Massachusetts from 1991 to 2005. The Econamine FG Plus^{SM} process used MEA-based solvent and achieved a capture rate between 85% and 95% for 40 MW gas.[21] The plant was shut down because of the high price of natural gas at the time. Several pilot-plant campaigns using monoethanolamine (MEA) were also performed at the CO_2 Technology Centre Mongstad (TCM) to study the performance at low CO_2 concentration (~3.7%).[16−20,22] This paper reports the pilot plant absorber performance and modeling results using PZAS with advanced intercooling with 4.3% CO_2 to demonstrate feasibility for the gas turbine application.

2. METHODOLOGY

2.1. Pilot Plant Overview. The Pilot Solvent Test Unit (PSTU) at the NCCC was modified to test PZAS with 4.3 dry mol % CO_2. The flue gas pretreatment and PZAS process are shown in Figure 1. Coal-fired flue gas containing about 11 mol % CO_2 was fed to a NaOH scrubber to remove SO_2. The gas was then diluted with air to reduce the CO_2 to about 4.3 mol % to simulate NGCC flue gas. The diluted gas could be cooled in the direct contact cooler (DCC) and saturated with water at 40 °C or sent directly to the absorber. In bypass mode, the flue gas was heated to 78 °C by the blower to partially simulate hot NGCC gas conditions. Both simple in-and-out and advanced pump-around intercooling were tested. Figure 2 shows the three absorber configurations: (A) absorber with in-and-out intercooling and DCC, (B) with pump-around intercooling and DCC, and (C) with pump-around intercooling but no DCC. When the DCC was online, the mixed gas was cooled and saturated with water at 40 °C, and when it was bypassed, the gas was heated to 78 °C and fed directly to the absorber column.

The absorber column has three beds of packing, but the top bed was not used for absorption. For the in-and-out cooling loop, solvent was removed from the bottom of the middle bed, intercooled, and returned to the top of the bottom bed. For the pump-around, solvent was recycled from the bottom of the third bed, cooled, and fed to the top of the third bed.

The flue gas flowed upward in the absorber and counter-currently contacted the solvent. The CO_2-scrubbed gas was washed with water to remove entrained solvent and control amine emissions and then vented. The rich solvent leaving the absorber bottom was pumped to the stripper for regeneration. The solvent was split into cold rich bypass and warm rich bypass for heat recovery. After two cross exchangers, the rich stream was heated to 150−155 °C by a steam heater. The bypass stream was fed to the stripper to condense the water vapor and recover the latent heat in the stripper overhead.

DOI: 10.1021/acs.iecr.9b05733
Ind. Eng. Chem. Res. 2020, 59, 7174−7181

Table 1 summarizes the detailed specifications of the test facilities.

Table 1. Summary of Equipment Specifications

	parameter	comments
absorber	column inner diameter (m)	0.66
	packing height (m)	2 × 6.10
	packing type	M252Y
	material	stainless steel
stripper	packing height (m)	2 × 2
	packing type	RSR #0.5, #0.7
	material	stainless steel
	cold cross exchanger area (m^2)	114.0
	hot cross exchanger area (m^2)	31.9
	cold rich exchanger area (m^2)	8.5

2.2. Measurement Methods. The methods for measuring gas and solvent compositions were the same as the NCCC 2018 campaign described in previous papers.[10,11] The gaseous CO_2 was measured continuously by online nondispersive infrared (NDIR) analyzers. Liquid PZ and CO_2 were analyzed by online autotitration about every 70 min. Samples were collected daily and analyzed by gas chromatography (GC) and total inorganic carbon (TIC) analyzers for PZ and CO_2, respectively. Solvent density and viscosity were measured continuously by online flowmeters and viscometers and were used for calculating PZ and CO_2 concentration. The correlations were described previously.[10]

2.3. Modeling Methods. The rigorous "Independence" model in Aspen Plus was used to simulate the absorber performance. It consists of several submodels, including solvent properties and packing characterization. The "Independence" model includes physical properties, thermodynamics, and kinetics models regressed from bench-scale experiments. The thermodynamics were built in the electrolyte nonrandom two liquid (e-NRTL) framework.[2] The packing characterization model includes interfacial area and liquid- and gas-side mass transfer coefficients developed by Song[23] from pilot-scale measurements with various random and structured packings. All the model parameters were regressed independently.

3. RESULTS AND DISCUSSION

3.1. NGCC and Coal Flue gas. Table 2 shows the typical parameters of coal and NGCC flue gas.[24]

Gas emitted from a coal flue contains about 13 mol % CO_2, while that from a gas turbine contains only ~4 mol %. The first challenge of carbon capture from NGCC is associated with the low CO_2, which reduces the partial pressure driving force for absorption. For NGCC conditions, 90% removal requires a lean CO_2 partial pressure below 0.4 kPa, which is the same partial pressure required for about 97% removal for the coal case. This means the lean solvent needs more overstripping to provide adequate mass transfer driving force for the gas application. It also makes >99% capture more difficult for NGCC. For coal, it has been demonstrated feasible to achieve high removal with reasonable energy and economic penalties.[11,25] However, for NGCC flue gas, high CO_2 removal (95−99%) may experience a greater penalty or may even be infeasible.

Table 2. Typical Flue Gas Parameters[24]

	coal (supercritical pulverized coal)	NGCC (F-class)
CO_2 (mol %)	12.88	3.91
H_2O (mol %)	14.51	8.41
N_2 (mol %)	68.54	74.42
O_2 (mol %)	3.25	12.38
temperature (°C)	56	117
gross power (MW)	550	630
flow rate (kg/s)	601.5	1029.7
flow rate (kg/s/MW)	1.09	1.58

The second challenge for capturing CO_2 from NGCC flue gas is the absorber column size. The flue gas flow rate per unit of electricity for NGCC is more than 60% greater than for coal-fired flue gas, which requires a greater absorber diameter and increases the capital cost. For the NGCC application, the absorber dominates the total capital cost of the capture plant. Therefore, the absorber design and optimization become more important for NGCC.

The third challenge for the NGCC application is related to the low liquid to gas (L/G) ratio and the heat of absorption. The low CO_2 content requires significantly less solvent circulation. The column temperature is mainly determined by the gas. The benefits of simple in-and-out intercooling are diminished because it is the gas that carries most of the enthalpy into the column. Cooling the solvent at such a low flow rate is not effective. Therefore, pump-around intercooling becomes necessary because it enhances the solvent rate and increases the cooling ability of the solvent.

Along with these challenges, NGCC flue gas capture also provides opportunities for absorber optimization. The natural gas flue gas is "cleaner" than coal flue gas. There is no SO_2 or fly ash, so flue gas pretreating is less expensive. Second, the water content in NGCC flue gas is only about 8 mol %. The water balance in the absorber column can be maintained by running the water wash section at about 43 °C with 8% inlet water. A direct contact cooler (DCC) is not necessary to knock out excess water. By removing the DCC and using pump-around intercooling, the bottom section of the absorber serves the purposes of both cooling and capturing.

3.2. Pilot Plant Campaign Results. PZAS was tested for about 4 months and 2100 operating hours. The starting solvent inventory had 2120 operating hours from the 2018 NCCC campaign with coal flue gas. The steady-state runs were defined based on flue gas rate, CO_2 concentration, lean solvent flow, feed temperature, intercooling temperature, solvent loading, and CO_2 removal. Table 3 summarizes the pilot plant steady-

Table 3. Summary of NCCC 2019 Campaign Operating Conditions

parameter	value
CO_2 in flue gas (mol % dry)	4.0−4.3%
PZ molality (m)	3.5−5.6
flue gas rate (kg/s)	0.63−1.01
solvent rate (kg/s)	0.61−1.77
CO_2 removal	80.0−95.8%
lean loading (mol CO_2/mol alkalinity)	0.186−0.254
rich loading (mol CO_2/mol alkalinity)	0.364−0.410
absorber solvent inlet T (°C)	40.3−53.5
absorber gas inlet T (°C)	39.7−83.0
absorber intercooling T (°C)	34.9−42.6

DOI: 10.1021/acs.iecr.9b05733
Ind. Eng. Chem. Res. 2020, 59, 7174−7181

state conditions, and Table 4 shows four representative cases for the major operating conditions. The detailed experimental data are provided in the Supporting Information.

Table 4. Four Representative Cases for Major Operating Conditions Tested in 2019 Campaign

runs		6	11	23	64
gas inlet T	°C	39.9	40.0	80.0	77.7
gas outlet T	°C	44.8	43.1	44.0	51.3
solvent inlet T	°C	40.8	41.4	40.7	40.7
solvent outlet T	°C	44.1	49.7	46.3	46.4
intercooling configuration		IO	PA	PA	PA
IC HX 1 inlet T	°C		45.0	45.7	44.6
IC HX 1 outlet T	°C		40.1	40.0	35.1
IC HX1 flow	* 10^{-3} m^3/s		1.17	1.39	1.13
IC HX 2 inlet T	°C	46.9	44.9	45.6	44.4
IC HX 2 outlet T	°C	39.9	40.1	39.9	35.0
IC HX2 flow	* 10^{-3} m^3/s	1.45	1.16	1.39	1.13
solvent inlet	kg/s	1.60	0.93	1.49	1.22
solvent outlet	kg/s	1.64	0.95	1.51	1.26
gas inlet	kg/s	1.01	0.63	1.01	1.01
gas outlet	kg/s	0.96	0.60	0.99	0.97
CO_2 inlet	dry mol %	4.31	4.31	4.29	4.31
CO_2 outlet	dry mol %	0.40	0.18	0.24	0.43
PZ molality	m	4.2	5.6	4.9	5.0
lean loading	(mol CO_2/mol N)	0.241	0.228	0.239	0.230
rich loading	(mol CO_2/mol N)	0.384	0.388	0.381	0.408
removal	%	90.7	95.8	94.3	90.0

3.2.1. Material Balance. The CO_2 material balance was studied to check the consistency of measurements. Three CO_2 rates were calculated: CO_2 removed from the gas phase, CO_2 captured in the liquid phase, and stripper overhead production. The gas phase balance was based on inlet and outlet flowmeters and NDIR measurements. The solvent loading was calculated from density and viscosity measurements. The stripper overhead product was assumed to be pure CO_2. As shown in Figure 3, the liquid phase removal rate matches the overhead production rate. The gas phase removal rate is consistently 3% higher. The error bars show the standard deviation associated with all the measurements. The liquid rate shows the least uncertainty because of the good reproducibility of the online density and viscosity measurements. The greater uncertainty of the overhead production was caused by fluctuation in the flow rate.

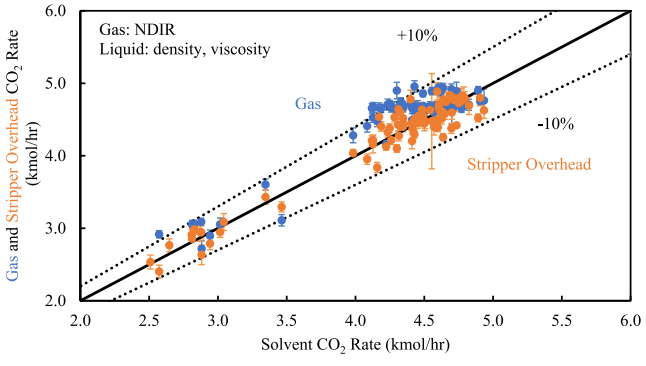

Figure 3. CO_2 transfer rate in the gas and liquid phases and the CO_2 production rate.

3.2.2. Absorber Performance. Data from 80 absorber steady-state runs were obtained over 2100 operating hours in 2019. The first 22 runs were parametric tests, which examined the absorber performance over a wide range of conditions, and the rest were from long-term testing designed to study the system stability, solvent oxidation, and other problems. There were four major absorber operating conditions tested during the campaign: in-and-out (40 °C) with 40 °C gas, pump-around (40 °C) with 40 °C gas, pump-around (40 °C) with 78 °C gas, and pump-around (35 °C) with 78 °C gas. The CO_2 removal (defined by eq 1) varied between 85% and 96% with lean loading from 0.19 to 0.25 mol CO_2/mol alkalinity. CO_2 penetration and number of transfer units (NTU) as defined in eq 2 were used to evaluate absorber performance.[11] The number of transfer units is used to capture the nonlinear increase in the transfer area required to achieve a high CO_2 removal. For example, if the mass transfer is controlled by gas film resistance, it takes twice as much packing area to achieve 99% removal (NTU = 4.6) as for 90% (NTU = 2.3). Usually the packing height or contacting area of a transfer unit (HTU) is approximately constant so the NTU is a useful transformation of experimental removal.

$$Removal = 1 - \frac{N_{out,CO_2}}{N_{in,CO_2}} \quad (1)$$

$$\mathrm{NTU} = -\ln(Penetration) = -\ln(1 - Removal) \quad (2)$$

Figure 4 shows the experimental absorber performance grouped with four operating conditions. The rich loading varied between 0.36 and 0.41, and it shows correlation with CO_2 penetration: the rich loading decreases from 0.4 to 0.38 as the removal increases from 90% to 95%. The delta loading reflects the energy penalty for high CO_2 removal at the NGCC condition. The long-term runs achieved rich loading exceeding 0.4, which is greater than the rich loading from the 2018 campaign at coal conditions.[11] This means that low CO_2 in the NGCC flue gas does not necessarily lead to a lower rich loading, nor to worse energy performance. This is because the column temperature is well-managed with pump-around intercooling, which increases the rich loading even at the low CO_2 partial pressure.

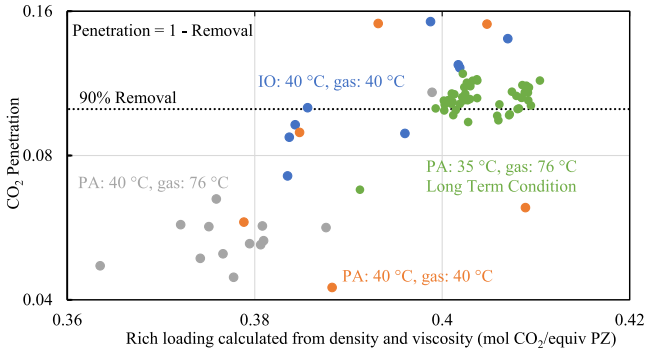

Figure 4. Experimental absorber performance for NCCC 2019 campaign (IO: in-and-out intercooling, PA: pump-around intercooling).

3.3. Model Results. *3.3.1. Model Validation.* The absorber performance was modeled rigorously using Aspen

DOI: 10.1021/acs.iecr.9b05733
Ind. Eng. Chem. Res. 2020, 59, 7174−7181

Plus. The CO_2 and PZ concentrations for model inputs were calculated from density and viscosity. The model underpredicts the absorber NTU by 46%, and the calculated PZ was increased by a factor of 1.08 to provide a better representation of the pilot plant data. This adjustment could be consistent with systematic analytical error or with systematic degradation of the solvent. Figure 5 compares the measured and modeled

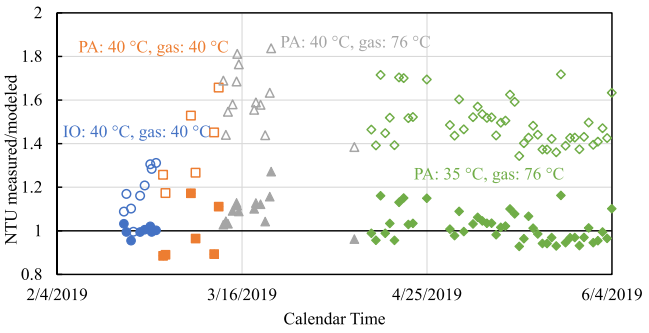

Figure 5. Absorber model validation for 2019 campaign. Points are color-coded for 4 major operating conditions. The hollow points are the raw model predictions, and the solid points are after the correction of PZ weight fraction.

absorber NTU in chronological order with color coding for the four major absorber conditions. The pump-around data are more scattered because the viscosity measurements showed a greater variation at these conditions. The relative difference in NTU between the model and the experiments shows a decreasing trend during the long-term testing, and it reflects the extent of solvent degradation. Figure 6 shows the NTU

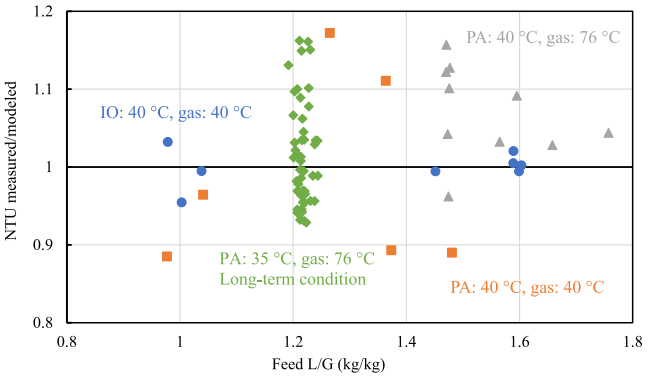

Figure 6. Comparison of experimental and modeled absorber NTU at variable L/G. Points are color-coated for different operating conditions.

ratio at different nominal L/G conditions (lean solvent rate to gas rate), and the model predictions are independent of L/G. Overall, the model is validated at different absorber configurations and operating conditions.

The measured temperature profile was also compared to the model predictions. Figures 7, 8, and 9 show results for 3 representative cases. In all figures, the temperature on the primary axis is plotted against the relative position, with 0 and 1 representing the top and bottom of the absorption column. The calculated CO_2 flux is shown on the secondary axis.

As shown in three figures, the shape of the temperature profile varies with the conditions of lean loading, L/G, and intercooling. At low lean loading and L/G, the gas carries the

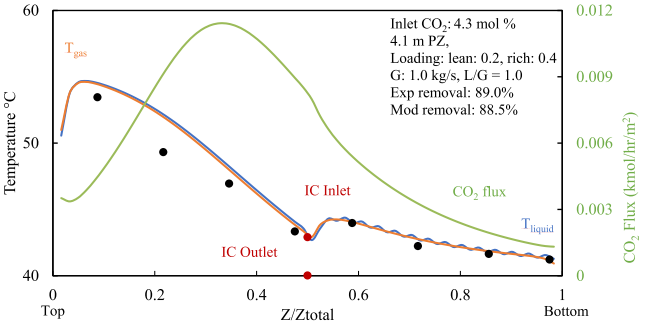

Figure 7. Absorber profile for in-and-out intercooling and 0.24 lean loading. Temperature measurements (points) and model predictions (curve) are shown on the primary axis; CO_2 transfer flux is shown on the secondary axis.

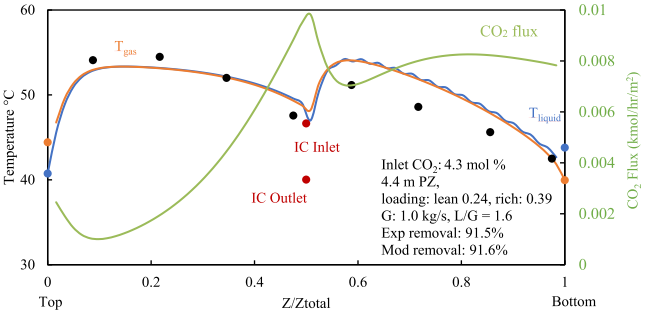

Figure 8. Absorber profile for in-and-out intercooling and 0.24 lean loading. Temperature measurements (points) and model predictions (curve) are shown on the primary axis; CO_2 transfer flux is shown on the secondary axis.

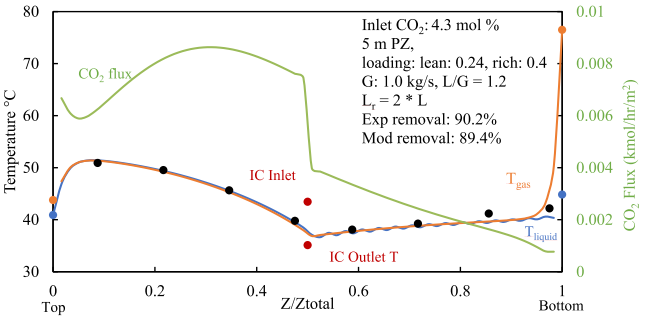

Figure 9. Absorber profile for pump-around intercooling and 0.24 lean loading. Temperature measurements (points) and model predictions (curve) are shown on the primary axis; CO_2 transfer flux is shown on the secondary axis.

heat of absorption, pushes the temperature bulge to the top of the column, and leads to a cold bottom. 90% removal is achievable because the overstripped solvent provides adequate CO_2 driving force even at elevated temperature, and the rich loading is high because of the cold rich temperature. Therefore, the low lean loading leads to a greater solvent capacity and can reduce the solvent circulation significantly.

With 0.24 lean loading and in-and-out intercooling (Figure 8), more solvent is needed to achieve 90% CO_2 removal. At the same time, the solvent pushes the reaction heat into the bottom of the column, but the simple in-and-out intercooling cannot cool the gas effectively given the L/G ratio, and the rich loading decreases at this high temperature. This leads to a

DOI: 10.1021/acs.iecr.9b05733
Ind. Eng. Chem. Res. 2020, 59, 7174−7181

significant increase of solvent circulation (about 50%) compared to 0.20 lean loading.

With pump-around intercooling, the solvent rate in the bottom section can be enhanced to provide effective cooling. As shown in Figure 9, the solvent rate in the bottom section is 2 times greater than the top. At this solvent rate, the intercooling is sufficient, and the temperature is low even with a hot flue gas inlet. As a result, the pump-around intercooling increases the rich loading and reduces the solvent requirement by 30% compared to in-and-out.

Generally, the temperature bulge at NGCC conditions tends to occur on the top section, given the low L/G. The maximum temperature is less than 55 °C (near the top), which is much lower than the maximum in coal conditions (about 68 °C near the bottom). At NGCC conditions, the heat generated per volume (or mass) gas is only a third of that at coal conditions; thus, the column temperature is generally lower. This is beneficial because it reduces the solvent equilibrium CO_2 pressure, compensating for the low CO_2 concentration, and increases the rich loading and solvent cyclic capacity.

3.3.2. Insights from the Model. 3.3.2.1. Effect of CO_2 Penetration. Along with the validated absorber model, the effects of CO_2 penetration, intercooling, and lean loading are evaluated in this section. At constant lean loading, the delta loading is a direct indicator of the energy performance. Given fixed CO_2 removal, delta loading is inversely proportional to solvent circulation: the greater delta loading means less solvent, thus less sensitive heat loss through cross exchangers. At greater rich loading, the stripper also performs better because CO_2 can be stripped more easily when the solvent has a greater equilibrium partial pressure. Figure 10 shows the

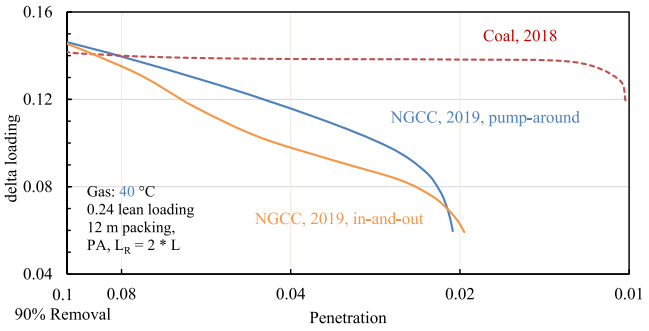

Figure 10. Solvent delta loading as a function of CO_2 penetration for absorber with coal[11] (red dashed line, in-and-out) and NGCC flue gas with pump-around (blue line) and in-and-out (orange line).

delta loading as a function of penetration for NGCC and coal conditions. The coal conditions were validated with the data from the 2018 NCCC campaign. At 90% removal, the NGCC shows a greater delta loading than coal, even though the CO_2 concentration is three times less. At NGCC conditions, the absorber temperature bulge tends to move to the top, and the rich solvent is colder than at coal conditions, which compensates for the low CO_2 partial pressure. Therefore, the energy performance is even better than coal. However, the delta loading at NGCC conditions shows a strong dependence on CO_2 penetration. At low CO_2, the energy performance is sensitive to removal, and the energy penalty is significant at high removal. The NGCC curve starts to bend at 0.024 penetration, where the equilibrium driving force at the lean end is depleted and a higher removal rate becomes impossible. On the other hand, the coal curve is almost flat for penetration between 0.1 to 0.013 and bends at a removal greater than 98%.

The delta loading and energy penalty for high CO_2 removal is less at higher CO_2 concentration. The temperature bulge affects the ability to reach high removal: at NGCC conditions, the temperature bulge moves to the top, and it increases the solvent equilibrium partial pressure at the lean end; but for coal, the top section at high removal is cold so it is easier to achieve high removal. If the CO_2 removal for the NGCC and coal capture system were both optimized, the optimal removal at NGCC would be lower than that at coal conditions.

3.3.2.2. Effect of Pump-around and in-and-out Intercooling. Pump-around and in-and-out intercooling are also compared in Figure 10. At 40 °C gas inlet and intercooling temperature, the delta loading of pump-around intercooling is generally greater than in-and-out. With enhanced solvent recycle, pump-around is able to cool the rich end and to increase the equilibrium rich loading, except with removal below 90% or greater than 98%. When the removal is low, the bottom of the column is cold because the low L/G leads to a temperature bulge at the top, so the benefits are not significant. At high removal, L/G increases, making cooling by in-and-out sufficient, and the solvent back-mixing caused by pump-around overshadows the cooling effect.

3.3.2.3. Effect of Gas Temperature and Intercooling Temperature. The effects of gas feed temperature and intercooling temperature are shown in Figure 11. Two gas

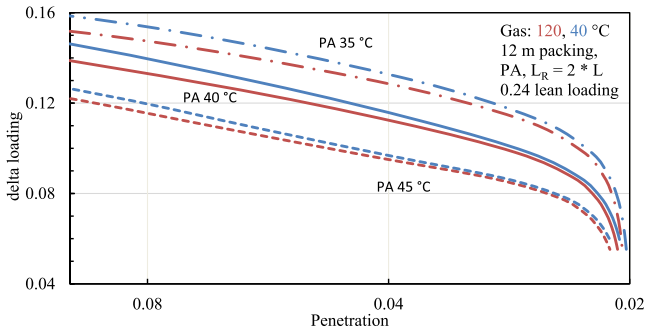

Figure 11. Absorber delta loading as a function of CO_2 penetration with pump-around intercooling at 35 °C (dash dot), 40 °C (solid line), and 45 °C (dashed line). Gas feed temperatures are 40 °C (blue) and 120 °C (red).

temperatures of interest are 40 and 120 °C. The 40 °C gas is saturated with water (7 mol %) to represent the DCC upstream, and the 120 °C gas contains 8 mol % water as a result of stoichiometry combustion of natural gas. The difference in delta loading between the 40 and 120 °C curves therefore represents the delta loading and energy penalty for taking out the DCC column, and it is less than 5%. This is because the 120 °C case is undersaturated with water and has a low enthalpy. It picks up water in the bottom of the absorber and is cooled quickly. The gas temperature only has a minor effect on the absorber performance. The water balance can also be maintained for the undersaturated flue gas by running the water wash at about 42 °C so that the CO_2 gas leaving the absorber has the same amount of water as the inlet.

The intercooling temperature, on the other hand, affects the absorber significantly. The delta loading can be enhanced by 10% when the intercooling temperature is reduced by 5 °C. The temperature in the bottom section is primarily set by the

DOI: 10.1021/acs.iecr.9b05733
Ind. Eng. Chem. Res. 2020, 59, 7174−7181

pump-around temperature, and it can dramatically change the equilibrium rich loading. Therefore, running colder is especially beneficial for pump-around intercooling. A similar effect of intercooling temperature was also found in absorption systems using MEA.[22]

3.3.2.4. Effect of Lean Loading. Figure 12 shows the absorber performance at 0.2 and 0.24 lean loading for both in-and-out and pump-around intercooling. The rich loading for pump-around cases is about the same, and the lower lean loading increases the solvent capacity by about 30%. The lower lean loading also leads to a greater maximum removal because it provides greater CO_2 transfer driving force at the lean end. At low lean loading, in-and-out performance is better than pump-around because the temperature bulge moves to the absorber top at this low L/G condition and the extra cooling at the bottom becomes marginal. The energy consumption for getting lower lean loading is greater because more water vapor will be stripped out, but the advanced stripper is capable of recovering the heat from water vapor in the stripper overhead. For PZ, operating at low lean loading could be risky because of solid precipitation, but during the 2018 and 2019 campaigns, the system was operated at a lean loading of 0.19 without precipitation.

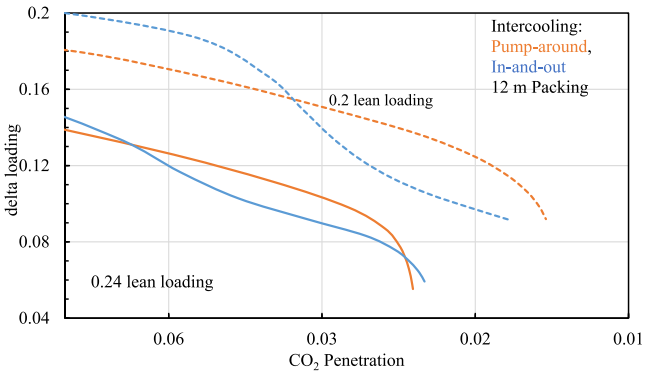

Figure 12. Absorber delta loading as a function of CO_2 penetration with pump-around (orange) and in-and-out (blue) intercooling at 0.2 (dashed line) and 0.24 (solid line) lean loadings. The gas feed temperatures for the pump-around and in-and-out are 120 and 40 °C, respectively.

4. CONCLUSION

A rigorous PZ absorber model has been validated using the steady-state data from the NCCC 2019 campaign at NGCC conditions. The operating conditions included lean loading (0.19−0.25 m CO_2/mol alkalinity), gas temperature (40, 78 °C), and intercooling temperature (35, 40 °C). With 12 m of packing and intercooling, CO_2 removal from 82% to 96% was achieved using 5 m PZ. The model is able to predict the absorber NTU and temperature profile accurately for both in-and-out and pump-around intercooling.

1. The delta loading at NGCC conditions for 90% removal is greater than the coal conditions although the CO_2 concentration is lower. This is because of low temperature in the absorber, especially the bottom, and it is low for two reasons:
    a. At low CO_2 concentration, there is less heat generated per mass gas, so the magnitude of the temperature bulge is smaller.
    b. At low L/G, gas tends to push the heat to the top of the column, so the bottom remains cold, which reduces the solvent equilibrium CO_2 partial pressure and increases the rich loading.
2. At NGCC conditions, high CO_2 removal leads to a greater penalty in the delta loading compared to coal conditions. The CO_2 transfer driving force will be depleted at the lean end because of the low CO_2 partial pressure and the high temperature.
3. Pump-around intercooling is almost always better than in-and-out at NGCC conditions because it cools the gas effectively with an enhanced solvent flow. With pump-around intercooling, the delta loading penalty for removing the DCC column is less than 5%.
4. At NGCC conditions, the absorber bottom temperature is dominated by the intercooling temperature, and lowering that temperature can improve the performance dramatically: reducing the intercooling temperature by 5 °C increases the delta loading by 10%.

Because of the low CO_2 concentration and high gas rate at NGCC conditions, the absorber dominates the total capital cost of the capture plant. With a fast solvent such as PZ, the absorber performance is not degraded at low CO_2 concentration because the column can be cooled effectively with intercooling. Therefore, PZ is excellent for the NGCC application because it reduces the packing requirements and the absorber cost.

■ ASSOCIATED CONTENT

Supporting Information

The Supporting Information is available free of charge at https://pubs.acs.org/doi/10.1021/acs.iecr.9b05733.

Experimental runs (PDF)

■ AUTHOR INFORMATION

Corresponding Author

*E-mail: gtr@che.utexas.edu.

ORCID

Gary T. Rochelle: 0000-0003-2887-356X

Notes

The authors declare no competing financial interest.

■ ACKNOWLEDGMENTS

Financial support was provided by the CO_2 Capture Project and the U.S. Department of Energy, Office of Fossil Energy through the CCSI^2 project (Carbon Capture Simulation for Industry Impact) (subcontract 318779 with Los Alamos National Laboratory). Aspen Plus proprietary software was provided by an academic license from AspenTech. AspenTech and Aspen Plus are trademarks of Aspen Technology, Inc. All rights reserved. Operational support for the pilot plant was provided by the team of the National Carbon Capture Center of Southern Company.

■ REFERENCES

(1) EPA *Inventory of U.S. Greenhouse Gas Emissions and Sinks*; 2019.
(2) Frailie, P. T. *Modeling of Carbon Dioxide Absorption/Stripping by Aqueous Methyldiethanolamine/Piperazine*, Ph.D. Dissertation, The University of Texas at Austin, 2014.
(3) Sachde, D.; Chen, E.; Rochelle, G. T. Modeling Pilot Plant Performance of an Absorber with Aqueous Piperazine. *Energy Procedia* **2013**, *37*, 1987−2001.

DOI: 10.1021/acs.iecr.9b05733
Ind. Eng. Chem. Res. 2020, 59, 7174−7181

(4) Rochelle, G. T.; Chen, E.; Freeman, S.; Van Wagener, D.; Xu, Q.; Voice, A. Aqueous piperazine as the new standard for CO_2 capture technology. *Chem. Eng. J.* **2011**, *171* (3), 725−733.
(5) Chen, E.; Fulk, S.; Sache, D.; Lin, Y.; Rochelle, G. T. Pilot Plant Activities with Concentrated Piperazine. *Energy Procedia* **2014**, *63*, 1376−1391.
(6) Zhang, Y.; Sachde, D.; Chen, E.; Rochelle, G. Modeling of absorber pilot plant performance for CO_2 capture with aqueous piperazine. *Int. J. Greenhouse Gas Control* **2017**, *64*, 300−313.
(7) Pun, B.; Jadhav, R.; Selinger, J.; Rochelle, G. *In Advancing CO_2 Capture from Natural Gas Combined Cycle with Piperazine Scrubbing, 14th Greenhouse Gas Control Technologies Conference Melbourne* **2018**, 21−26.
(8) Lin, Y.-J.; Chen, E.; Rochelle, G. T. Pilot plant test of the advanced flash stripper for CO_2 capture. *Faraday Discuss.* **2016**, *192*, 37−58.
(9) Zhang, Y. *Absorber and Aerosol Modeling in Amine Scrubbing for Carbon Capture*. Ph.D. Dissertation, The University of Texas at Austin, 2018.
(10) Rochelle, G. T.; Wu, Y.; Chen, E.; Akinpelumi, K.; Fischer, K. B.; Gao, T.; Liu, C.-T.; Selinger, J. L. Pilot plant demonstration of piperazine with the advanced flash stripper. *Int. J. Greenhouse Gas Control* **2019**, *84*, 72−81.
(11) Gao, T.; Selinger, J. L.; Rochelle, G. T. Demonstration of 99% CO_2 removal from coal flue gas by amine scrubbing. *Int. J. Greenhouse Gas Control* **2019**, *83*, 236−244.
(12) Morgan, J. C.; Soares Chinen, A.; Omell, B.; Bhattacharyya, D.; Tong, C.; Miller, D. C.; Buschle, B.; Lucquiaud, M. Development of a Rigorous Modeling Framework for Solvent-Based CO_2 Capture. Part 2: Steady-State Validation and Uncertainty Quantification with Pilot Plant Data. *Ind. Eng. Chem. Res.* **2018**, *57* (31), 10464−10481.
(13) Cansolv *Testing of Cansolv DC-201 CO_2 Capture System with Simulated Natural Gas Testing*; 2015.
(14) Sachde, D.; Rochelle, G. T. Absorber Intercooling Configurations using Aqueous Piperazine for Capture from Sources with 4 to 27% CO_2. *Energy Procedia* **2014**, *63*, 1637−1656.
(15) Zhang, Y.; Freeman, B.; Hao, P.; Rochelle, G. T. Absorber modeling for NGCC carbon capture with aqueous piperazine. *Faraday Discuss.* **2016**, *192*, 459−477.
(16) Mejdell, T.; Vassbotn, T.; Juliussen, O.; Tobiesen, A.; Einbu, A.; Knuutila, H.; Hoff, K. A.; Andersson, V.; Svendsen, H. F. Novel full height pilot plant for solvent development and model validation. *Energy Procedia* **2011**, *4*, 1753−1760.
(17) Faramarzi, L.; Thimsen, D.; Hume, S.; Maxon, A.; Watson, G.; Pedersen, S.; Gjernes, E.; Fostås, B. F.; Lombardo, G.; Cents, T.; Morken, A. K.; Shah, M. I.; de Cazenove, T.; Hamborg, E. S. Results from MEA Testing at the CO_2 Technology Centre Mongstad: Verification of Baseline Results in 2015. *Energy Procedia* **2017**, *114*, 1128−1145.
(18) Gjernes, E.; Pedersen, S.; Cents, T.; Watson, G.; Fostås, B. F.; Shah, M. I.; Lombardo, G.; Desvignes, C.; Fløe, N. E.; Morken, A. K.; de Cazenove, T.; Faramarzi, L.; Hamborg, E. S. Results from 30 wt% MEA Performance Testing at the CO_2 Technology Centre Mongstad. *Energy Procedia* **2017**, *114*, 1146−1157.
(19) Brigman, N.; Shah, M. I.; Falk-Pedersen, O.; Cents, T.; Smith, V.; De Cazenove, T.; Morken, A. K.; Hvidsten, O. A.; Chhaganlal, M.; Feste, J. K.; Lombardo, G.; Bade, O. M.; Knudsen, J.; Subramoney, S. C.; Fostås, B. F.; de Koeijer, G.; Hamborg, E. S. Results of Amine Plant Operations from 30 and 40 wt % Aqueous MEA Testing at the CO_2 Technology Centre Mongstad. *Energy Procedia* **2014**, *63*, 6012−6022.
(20) Hamborg, E. S.; Smith, V.; Cents, T.; Brigman, N.; Pedersen, O. F.; De Cazenove, T.; Chhaganlal, M.; Feste, J. K.; Ullestad, Ø.; Ulvatn, H.; Gorset, O.; Askestad, I.; Gram, L. K.; Fostås, B. F.; Shah, M. I.; Maxson, A.; Thimsen, D. Results from MEA testing at the CO_2 Technology Centre Mongstad. Part II: Verification of baseline results. *Energy Procedia* **2014**, *63*, 5994−6011.
(21) Reddy, S.; Gilmartin, J. In *Fluor's Econamine FG PlusSM Technology for Post Combustion CO_2 Capture, GPA Gas Treatment Conference*, Amsterdam, The Netherlands, 2008.
(22) Tobiesen, F. A.; Svendsen, H. F.; Mejdell, T. Modeling of Blast Furnace CO_2 Capture Using Amine Absorbents. *Ind. Eng. Chem. Res.* **2007**, *46* (23), 7811−7819.
(23) Song, D. *Effect of Liquid Viscosity on Liquid Film Mass Transfer for Packings*. Ph.D. Dissertation, The University of Texas at Austin, 2017.
(24) NETL *Cost and Performance Baseline for Fossil Energy Plants Volume 1a: Bituminous Coal (PC) and Natural Gas to Electricity Revision 3*; 2015.; DOI: 10.2172/1480987.
(25) Nakagami, Y.; Nojo, T.; Hirata, T.; Tsujiuchi, T.; Kamijo, T.; Kishimoto, S.; Kawasaki, S. In *Near-Zero Emission Thermal Power Plant using Advanced KM CDR Process™, Post Combustion Capture Conference 5, Kyoto, Japan*, Kyoto, Japan, 2019.

DOI: 10.1021/acs.iecr.9b05733
Ind. Eng. Chem. Res. 2020, 59, 7174−7181